

Beyond immune escape: a variant surface glycoprotein causes suramin resistance in *Trypanosoma brucei*

Natalie Wiedemar,^{1,2} Fabrice E. Graf,^{1,2†}
Michaela Zwyer,^{1,2} Emiliana Ndomba,^{1,2‡}
Christina Kunz Renggli,^{1,2} Monica Cal,^{1,2}
Remo S. Schmidt,^{1,2} Tanja Wenzler^{1,2§} and
Pascal Mäser ^{1,2*}

¹Swiss Tropical and Public Health Institute, Basel CH-4002, Switzerland.

²University of Basel, Basel CH-4001, Switzerland.

Summary

Suramin is one of the first drugs developed in a medicinal chemistry program (Bayer, 1916), and it is still the treatment of choice for the hemolymphatic stage of African sleeping sickness caused by *Trypanosoma brucei rhodesiense*. Cellular uptake of suramin occurs by endocytosis, and reverse genetic studies with *T. b. brucei* have linked downregulation of the endocytic pathway to suramin resistance. Here we show that forward selection for suramin resistance in *T. brucei* spp. cultures is fast, highly reproducible and linked to antigenic variation. Bloodstream-form trypanosomes are covered by a dense coat of variant surface glycoprotein (VSG), which protects them from their mammalian hosts' immune defenses. Each *T. brucei* genome contains over 2000 different VSG genes, but only one is expressed at a time. An expression switch to one particular VSG, termed VSG^{Sur}, correlated with suramin resistance. Reintroduction of the originally expressed VSG gene in resistant *T. brucei* restored suramin susceptibility. This is the first report of a link between antigenic variation and drug resistance in African trypanosomes.

Introduction

Sleeping sickness, also called human African trypanosomiasis (HAT), is still a prevalent disease in sub-Saharan Africa. It is transmitted by the blood-feeding tsetse flies and caused by two subspecies of *Trypanosoma brucei*: *T. b. gambiense* causes the chronic form, *T. b. rhodesiense* the acute form of HAT. Untreated, both typically end with coma and death. Among the four currently available drug therapies, suramin is the oldest one and is used for the treatment of the first, hemolymphatic stage of *T. b. rhodesiense* HAT. Suramin is a big and highly charged molecule (Supporting Information Fig. S1) and therefore not able to passively diffuse through biological membranes. It is supposedly taken up by receptor-mediated endocytosis (Fairlamb and Bowman, 1980) with an involvement of low-density lipoprotein (Vansterkenburg *et al.*, 1993). More recent high-throughput RNAi-screens (Alsford *et al.*, 2012) have shown a variety of endosomal and lysosomal genes to render trypanosomes less susceptible to suramin when knocked-down, which is in agreement with an uptake via endocytosis. Furthermore, knock-down of the invariant surface glycoprotein ISG75 led to a 50% reduction of suramin susceptibility. ISG75 was therefore proposed to be the binding partner of suramin on the cell surface (Alsford *et al.*, 2012, 2013). The mode of action of suramin has been elusive since it was shown to have diverse intracellular targets (Wang, 1995).

Despite its use for about a hundred years now, there have been no reports of suramin resistance in human pathogenic trypanosomes. The cure-rates of first stage *T. b. rhodesiense* HAT are typically high. Suramin treatment failures were mainly observed in context of a miss-staging of the disease (Pépin and Milord, 1994), since suramin has a low brain permeability and is ineffective once the trypanosomes have crossed the blood-brain barrier. However, suramin resistance is prevalent among animal pathogenic trypanosomes, for example in *T. evansi* isolates from Sudanese camels (El Rayah *et al.*, 1999) and Chinese buffaloes and mules (Zhou *et al.*, 2004). Selection for suramin resistance is feasible under laboratory conditions. After 550 days of *in vitro* selection *T. evansi* were 1800-fold less susceptible to suramin

Accepted 27 September, 2017. *For correspondence. E-mail pascal.maeser@unibas.ch; Tel. (+41) 61 284 8338; Fax (+41) 61 284 8101 Present addresses: [†]Department of Chemistry and Molecular Biology and Centre for Antibiotic Resistance Research (CARE), University of Gothenburg, Gothenburg 405 30, Sweden. [‡]Ifakara Health Institute, Ifakara, Tanzania [§]University of Bern, Bern, CH-3000, Switzerland.

(Fang *et al.*, 1994), and *T. brucei* showed a resistance factor of 20–140 after *in vivo* selection with subcurative doses (Scott *et al.*, 1996). The suramin resistance phenotype was lost after transformation of the trypanosomes to insect-stage, procyclic forms.

We have observed the appearance of strong drug resistance in *T. brucei* bloodstream forms after exposure to high suramin concentrations for only a few days. Here, we use transcriptomics and reverse genetics to elucidate the genetic mechanism behind this phenomenon.

Results

In vitro selection for suramin resistance monitored in real-time

Isothermal microcalorimetry allows to monitor the growth of axenic *T. brucei* cultures in real-time based on the heat emitted by the cells' metabolism (Wenzler *et al.*, 2012). Here, we use the technology to track the emergence of drug resistance. Incubated at presumably lethal concentrations of suramin, i.e., the 5-fold and 25-fold of the IC_{50} , *T. b. rhodesiense* bloodstream-form cultures appeared to be dead after two days, started to regrow after three, and had fully recovered by day five (Fig. 1). This phenomenon was consistently observed: we have performed the same experiment with *T. b. brucei*, which also recovered from suramin pressure within one week. In all cases, the recovered trypanosomes were suramin-resistant by factors between 30 and 100 as compared to the starting population. No such phenomenon was observed with other drugs: melarsoprol or pentamidine completely killed the *T. brucei* cultures at

concentrations of 5- and 25-fold their IC_{50} (Wenzler *et al.*, 2012) (Fig. 1).

Rapid emergence of resistance also in clonal populations

The microcalorimetric experiment was performed with an inoculum of 10^5 cells. To rule out that a subpopulation of suramin-resistant trypanosomes had been present all along and was simply selected for under drug pressure, we repeated the experiment with fresh *T. b. rhodesiense* STIB900 clones. Incubated at concentrations between 500 and 1700 nM suramin (i.e., 5–80 fold their respective IC_{50}), drug-resistant progeny was again obtained within one week for all tested clones [$n = 11$]. Table 1 summarizes the results for one clone (named *T. b. rhodesiense* STIB900_c1) and four independent suramin-resistant derivatives thereof (named *T. b. rhodesiense* STIB900_c1_sur1 to _sur4), selected at 1050 nM suramin (80-fold the IC_{50}). All four derivatives were at least 90-fold resistant to suramin as compared to the parent clone STIB900_c1 ($p < 0.0001$ by One Way ANOVA with Tukey's multiple comparisons test). While their sensitivity to melarsoprol and pentamidine was unchanged (Table 1), the suramin-resistant lines were cross-resistant to the structurally related trypanocidal dye trypan blue ($p < 0.001$, Ehrlich, 1904; Supporting Information Fig. S1). The cross-resistance phenotype was stable in the absence of drug pressure for several weeks. After 80 days of cultivation, however, the resistance factor had decreased to 10- to 50-fold in the four lines (Fig. 2). Cumulative growth curves (Supporting Information Fig. S2) demonstrate slightly longer population doubling times of the resistant derivatives (8.2 h for

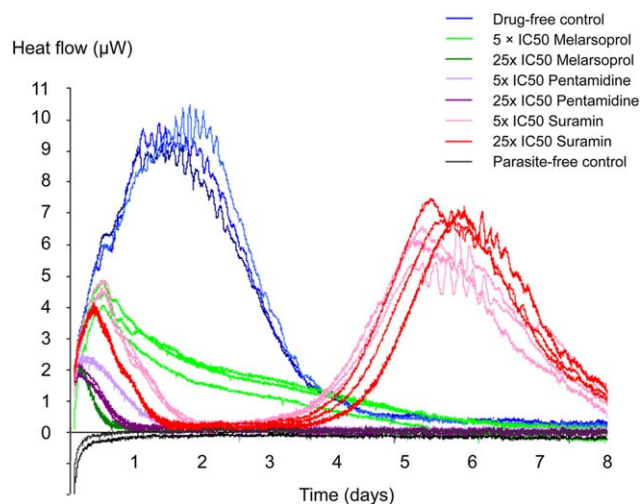


Fig. 1. Bloodstream-form *T. brucei* incubated with presumably lethal concentrations of suramin rapidly became resistant and regrew. No such phenomenon was observed with the drugs melarsoprol or pentamidine.

Table 1. Drug sensitivities of the parental clone *T. b. rhodesiense* STIB900_c1 and four independently selected derivatives (sur1–4). Values are 50% inhibitory concentrations in nM \pm standard deviation ($n \geq 5$)

	Suramin	Trypan Blue	Melarsoprol	Pentamidine
STIB900_c1	13 \pm 4	2700 \pm 900	22 \pm 1.2	1.1 \pm 0.4
STIB900_c1_sur1	1250 \pm 40	16,200 \pm 5600	23 \pm 2.3	1.0 \pm 0.3
STIB900_c1_sur2	1240 \pm 10	16,300 \pm 5300	24 \pm 1.9	1.5 \pm 1.1
STIB900_c1_sur3	1240 \pm 90	16,300 \pm 5200	24 \pm 2.2	1.2 \pm 0.5
STIB900_c1_sur4	1270 \pm 100	16,600 \pm 5700	26 \pm 3.3	1.5 \pm 1.2

STIB900_c1_sur1 and 8.3 h for STIB900_c1_sur4) as compared to the suramin sensitive parent clone (7.7 h).

VSGs are differentially expressed in resistant and sensitive parasites

The finding that suramin resistance reproducibly developed even in cultures from freshly cloned trypanosomes, indicated that the underlying mutation – whatever its nature – had occurred during the selection period. However, the reproducible acquisition of a particular point mutation is unlikely to happen within days. We, therefore, reckoned the mechanism of suramin resistance more likely to be reflected at the level of gene expression than gene sequence. Total RNA from *T. b. rhodesiense* STIB900_c1 and the four selected lines, grown in the absence of suramin, was subjected to quantitative transcriptomics by mRNA-Seq. Over 50 million high-quality reads were obtained for each line (European Nucleotide Archive accession PRJEB20650). As

expected given the short interval between suramin-sensitive parent and suramin-resistant derivatives, there were hardly any differences in transcript abundance (Supporting Information Fig. S3). Genes encoding proteins that had been shown to be involved in suramin resistance in *T. brucei* (Alsford *et al.*, 2012), i.e., the invariant surface glycoprotein ISG75, the putative major facilitator superfamily transporter MFST or the lysosomal proteins CatL, CBP1 and GLP-1, were not differentially expressed in the suramin-resistant lines. The only hits that were differentially expressed mapped to *VSG* genes (Supporting Information Fig. S3). Thus all four selected lines had undergone an expression switch to a new *VSG*.

The suramin-resistant lines have all switched to the same VSG

The sequence of this newly expressed *VSG* was reconstructed by *de novo* assembly from the Illumina reads. The reconstructed sequence was verified by reverse transcriptase PCR followed by direct sequencing, making use of the fact that all *T. brucei* mRNAs possess the same spliced leader sequence at the 5' end (Parsons *et al.*, 1984). Three of the four resistant lines had switched to the identical *VSG* gene, which was termed *VSG^{Sur}* (GenBank accession MF093647). *T. b. rhodesiense* STIB900_c1_Sur2 expressed a gene that was almost identical to *VSG^{Sur}* (GenBank accession MF093648), differing only in four SNPs (two of which were non-synonymous) and a different 3' UTR. The sequence of the *VSG* expressed in the parental clone STIB900_c1 was reconstructed in the same way and termed *VSG⁹⁰⁰* (GenBank accession MF093646). Re-mapping of the Illumina reads upon inclusion of these two *VSG* sequences resulted in more than 10% of reads mapping to *VSG⁹⁰⁰* in the sensitive parent clone, and more than 10% of reads mapping to *VSG^{Sur}* in all the resistant derivatives (Fig. 3). Reverse-transcriptase qPCR confirmed the switch from *VSG⁹⁰⁰* to *VSG^{Sur}* in the resistant lines as they all showed a more than 10,000-fold upregulation of *VSG^{Sur}* (Fig. 4). We also analyzed the suramin-selected derivatives of another

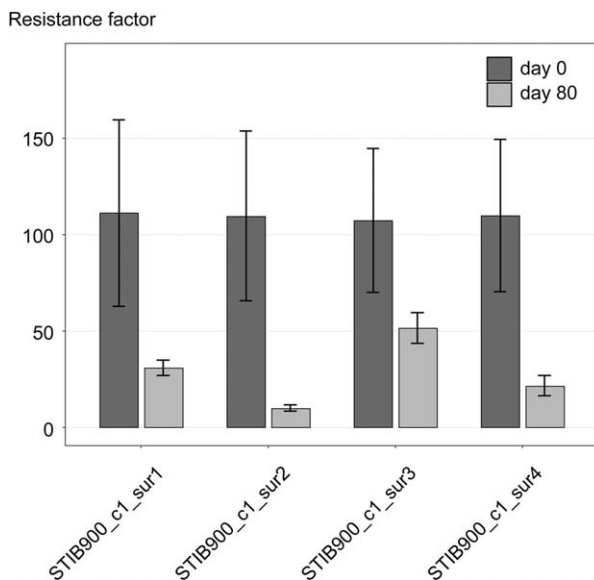


Fig. 2. Stability of suramin resistance in the absence of selection. The resistance factor was defined as the IC_{50} of the derivatives of *T. b. rhodesiense* STIB900_c1 divided by the IC_{50} of *T. b. rhodesiense* STIB900_c1 itself, grown in parallel.

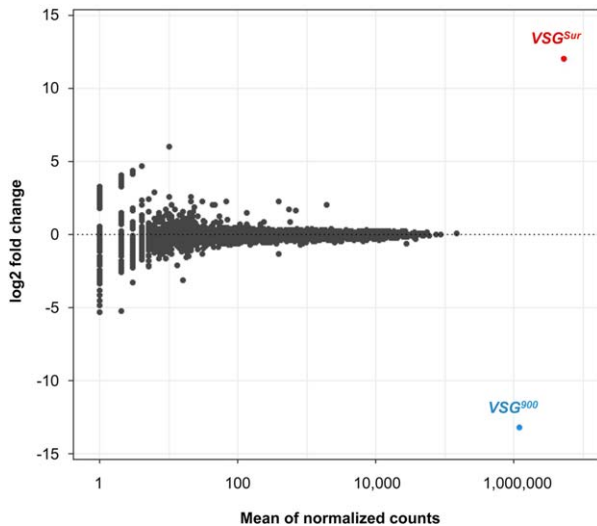


Fig. 3. Differential gene expression of resistant derivatives vs. suramin-sensitive parental *T. b. rhodesiense* STIB900 clone as analyzed with DESeq2. Illumina reads were mapped to the TREU927 reference genome supplemented with Lister 427 bloodstream expression sites and with the sequences of VSG^{Sur} and VSG^{900} . The x-axis displays transcript abundance (mean read count over all samples normalized for library size) and the y-axis displays the logarithmic fold-change of transcript abundance (all four resistant derivatives vs. the sensitive parent clone). Genes with a significant ($p < 0.01$) fold-change are colored in red if overexpressed, and in blue if underexpressed in the resistant derivatives.

clone of *T. b. rhodesiense* STIB900 (STIB900_c2), and they had switched to VSG^{Sur} as well (Fig. 4). Moreover, the suramin-resistant population derived from *T. b. brucei* strain BS221 had undergone a switch to a VSG with 97% nucleotide sequence identity (Needleman-Wunsch global alignment) to VSG^{Sur} (Fig. 4; GenBank accession MF093649).

Suramin resistance correlates with expression of VSG^{Sur} but not ESAG7

VSG^{Sur} encodes a bona fide variant surface glycoprotein of 491 amino acids with an N-terminal export signal and a C-terminal GPI-anchoring signal as predicted by SignalP (Nielsen *et al.*, 1997) and GPI-SOM (Fankhauser and Mäser, 2005), respectively. Profile scans against the Procite and Pfam databases of sequence motifs did not return significant hits beside the entry for the *T. brucei* VSG conserved C-terminal domain (PF10659; *E*-value of 0.0002). A Blastp search with VSG^{Sur} as the query against the non-redundant protein sequence database at NCBI returned significant hits on variant surface glycoproteins, the best one on VSG 522 (GenBank: AGH61081.1) with a sequence identity of 72%. The same search against all organisms other than

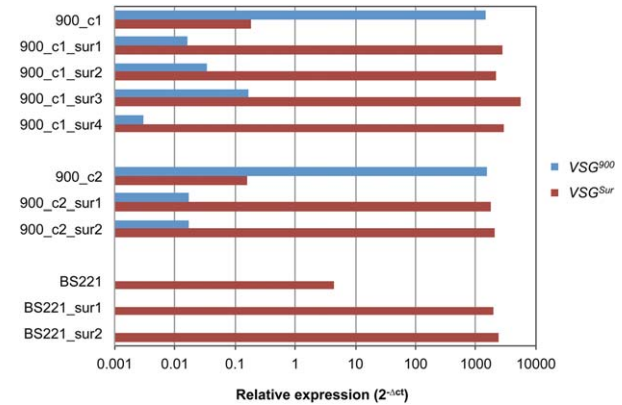


Fig. 4. Expression of VSG^{Sur} and VSG^{900} as determined by qRT-PCR in resistant *T. b. rhodesiense* and *T. b. brucei*, normalized to telomerase reverse transcriptase (*TERT*).

Trypanosoma spp. did not return a single hit. In the absence of any particular feature that would distinguish it from other VSGs, we initially presumed that it is not VSG^{Sur} itself that caused drug resistance but one of the expression site associated genes (*ESAGs*), which are polycistronically co-transcribed with each VSG and which could have failed to correctly map due to sequence divergence between STIB900 and the reference sequence used. If an antigenic switch results from activation of a new VSG expression site, new alleles of *ESAGs* will be expressed as well. If the switch is due to replacement of the active VSG by gene conversion, the expressed *ESAGs* will remain the same.

ESAG7 encodes the non-anchored part of the heterodimeric transferrin receptor and differs in sequence among the *T. brucei* VSG expression sites (van Luenen *et al.*, 2005; Hertz-Fowler *et al.*, 2008). For each of the five sequenced *T. b. rhodesiense* lines, the whole transcriptome was assembled *de novo* from the Illumina reads and the expressed *ESAG7* was extracted using a blast search (Tb927.7.3260, 2175 nt). Three of the suramin-resistant lines expressed exactly the same *ESAG7* gene as the parental *T. b. rhodesiense* STIB900_c1 (GenBank accession MF093650); the fourth expressed an *ESAG7* that differed in five nucleotides, two of which were non-synonymous (GenBank accession MF093651). Thus in one of the suramin-selected lines, the switch to VSG^{Sur} appears to have occurred by activation of a new expression site, while in the remaining three it happened by gene conversion, replacing the originally expressed VSG^{900} gene while maintaining the *ESAGs*. This strongly suggests that it is the expression of VSG^{Sur} itself, and not of the *ESAGs*, that causes suramin resistance. This hypothesis was corroborated by reverse genetic manipulation of VSG expression.

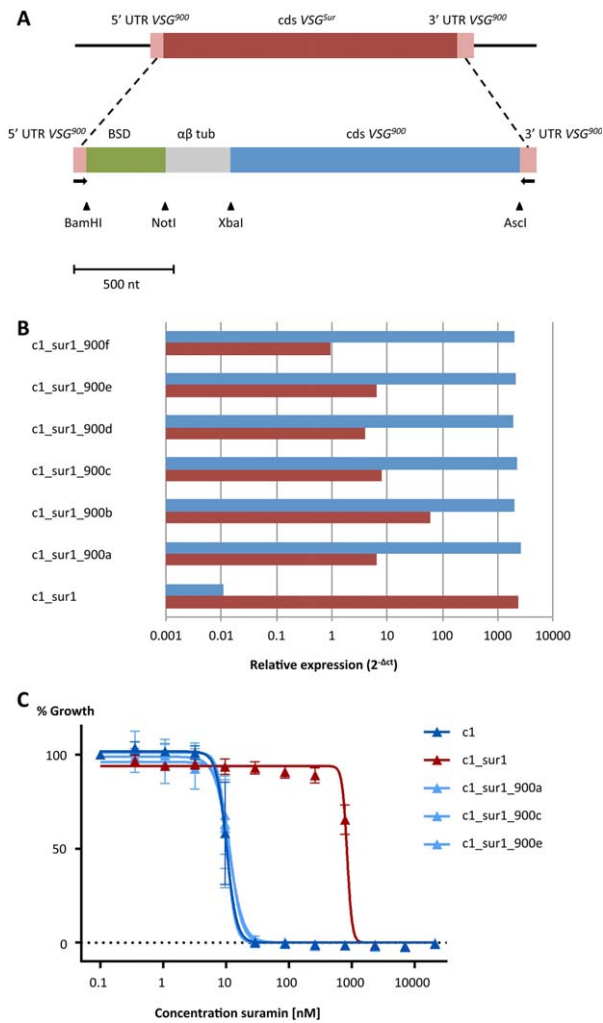


Fig. 5. Reverse genetic re-introduction of VSG^{900} . A) Schematic illustration of VSG^{Sur} (top) and the construct (bottom) used for re-introduction of VSG^{900} into the active bloodstream expression site of the resistant derivative STIB900_c1_sur1. The construct is framed with the 5' and 3' untranslated region (UTR) of VSG^{Sur} , it contains a blastocidin resistance gene (BSD), an $\alpha\beta$ tubulin splice site ($\alpha\beta$ tub) and the coding sequence (cds) of VSG^{900} . Binding sites of primers used for the verification of the genomic integration of the construct are indicated with black arrows. B) qRT-PCR, normalized with *TERT*. Expression of VSG^{Sur} (red) and VSG^{900} (blue) are shown for STIB900_c1_sur1 and six transfected clones thereof, with VSG^{900} introduced into the active bloodstream expression site. C) Suramin dose-response curves for STIB900_c1_sur1 and three transfected clones expressing VSG^{900} .

Reversal of the VSG^{900} - VSG^{Sur} switch restores suramin sensitivity

We made a genetic construct (Fig. 5A) to target the active VSG expression site of the suramin-resistant *T. b. rhodesiense* STIB900_c1_sur1. In order to exchange the expressed VSG^{Sur} with VSG^{900} , the construct was framed with the 5' and 3' UTR of VSG^{Sur} and contained the coding sequence of VSG^{900} together with a

blastocidin resistance gene. Positive transfectants were selected with blastocidin and cloned by limiting dilution. The construct had integrated in the genomes of all the analyzed clones [$n=6$] as determined by PCR using primers binding to the 5' and 3' UTR of VSG^{Sur} as the adjacent genomic context was unknown. Reverse-transcriptase qPCR confirmed a high expression of the re-introduced VSG^{900} (Fig. 5B). Subsequent drug sensitivity assays with three of the transfectants showed a complete loss of resistance in all of them, with IC_{50} values between 10 and 12 nM (Fig. 5C). One of the transfectants was once more subjected to suramin pressure. It quickly reestablished suramin resistance with a resistance level similar to STIB900_c1_sur1 (Fig. 6). Since these re-selected parasites could have undergone either expression site switch or gene conversion in order to re-express VSG^{Sur} , we investigated three lines selected from one transfectant by PCR using primers binding to the 5' and 3' UTR of VSG^{Sur} . Two of them (c1_sur1_900a_sur1 and c1_sur1_900a_sur2) had lost the construct, thus had undergone a gene conversion in order to switch back to VSG^{Sur} . In the third line (c1_sur1_900a_sur3) the construct was still present, therefore it had undergone an expression site switch in order to express VSG^{Sur} . We subsequently exposed the three lines to blastocidin; as expected the two lines that had undergone gene conversion were killed. The line that had undergone an expression site switch recovered under blastocidine pressure and the obtained parasites (c1_sur1_900a_sur3_bl1, _bl2 and _bl3) had completely lost the suramin resistance (Fig. 6).

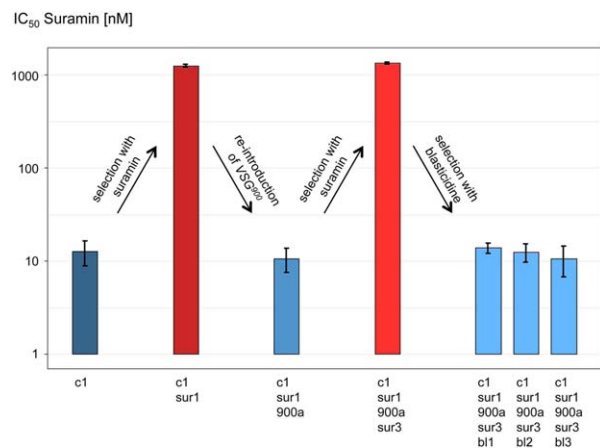


Fig. 6. Ups and downs of suramin sensitivity in the course of the experiment. IC_{50} values are shown for the sensitive parent clone c1 before selection (dark blue), one of the resistant derivatives after suramin selection (dark red), a transfected clone thereof with VSG^{900} re-introduced into the active bloodstream expression site (blue), one suramin selected derivative of that clone (light red), and three blastocidine selected lines thereof (light blue).

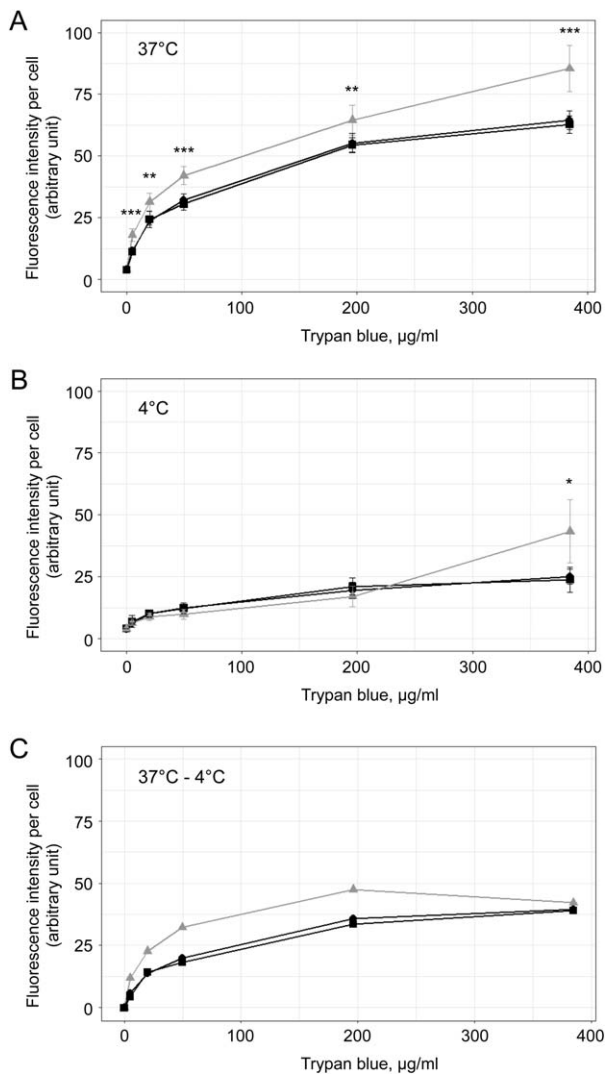


Fig. 7. Fluorescence of suramin sensitive and resistant cells incubated at different concentrations of trypan blue for two hours. Significantly different fluorescence levels between the sensitive and the resistant lines are indicated (*, $p < 0.05$; **, $p < 0.01$; ***, $p < 0.001$; $n \geq 5$, pairwise *t*-test); there were no significant differences between the two resistant lines. (A) Cells incubated at 37°C: the fluorescence levels represent surface bound plus endocytosed trypan blue. (B) Cells incubated at 4°C: the fluorescence levels represent surface-bound trypan blue. (C) The difference between the fluorescence at 37°C and 4°C therefore represents an estimate of the endocytosed trypan blue.

Binding and uptake of trypan blue

We exploited the facts that the suramin-selected lines were cross-resistant to trypan blue, and that trypan blue becomes fluorescent when bound to protein (Avelar-Freitas *et al.*, 2014), to further examine the observed phenomenon of drug resistance. The fluorescence of trypanosomes was quantified by flow cytometry after incubation for two hours with different concentrations of trypan blue (Fig. 7). Since dead cells are strongly

perfused by trypan blue, we first compared dead and living cells. The dead cells showed a much higher fluorescence and could be clearly separated from the living cells by setting the gate accordingly in a cell-size versus fluorescence plot (Supporting Information Fig. S4). Fluorescence of living cells incubated at physiological temperature is derived from both, surface bound and endocytosed trypan blue. At 37°C the two tested resistant derivatives (STIB900_c1_sur1 and STIB900_c1_sur4) showed significantly lower fluorescence levels when compared to the sensitive parent clone (STIB900_c1) over all concentrations (Fig. 7A). As endocytosis in trypanosomes is inactivated at low temperatures (Brickman *et al.*, 1995), we performed the same experiment at 4°C to quantify the fluorescence of surface-bound trypan blue (Fig. 4B). The resistant parasites showed similar levels of fluorescence as the sensitive clone at concentrations of 5–200 $\mu\text{g ml}^{-1}$ but significantly differed at 390 $\mu\text{g ml}^{-1}$, where the sensitive clone showed a strong increase in fluorescence. If the fluorescence at 37°C represents binding plus uptake, and the fluorescence at 4°C represents binding, then the curve obtained by subtraction (Fig. 7C) represents the trypan blue which had been endocytosed during the two hours of incubation. These values were lower for the resistant parasites than for the sensitive clone at concentrations up to 200 $\mu\text{g ml}^{-1}$. There was no difference at 390 $\mu\text{g ml}^{-1}$ trypan blue, possibly due to toxicity and inhibition of endocytosis in the sensitive clone.

Discussion

The famous parasitologist Frank Hawking (father of the even more famous physicist Stephen Hawking) stated that ‘Strains of trypanosomes may be made suramin-resistant in the laboratory, but this resistance takes much longer to develop than with arsenicals’ (Hawking, 1963). Here we show that >90-fold suramin resistance emerges in *T. brucei* spp. bloodstream forms after only few days of *in vitro* selection at high drug pressure. In contrast, it had taken us almost two years to select for melarsoprol-resistant derivatives of *T. b. rhodesiense* STIB900 with resistance factors of the same magnitude (Bernhard *et al.*, 2007). Comparative analysis of gene expression showed an association of a particular VSG with suramin resistance. Our first suspicion, that VSG^{Sur} was only a marker and the actual cause of resistance was one of the ESAGs, was rebutted by the finding that three of the four resistant lines had switched their VSG gene while maintaining the VSG expression site, as indicated by perfect conservation of expressed ESAG7. The finding that one of the resistant lines expressed a slightly different ESAG7 indicated that VSG^{Sur} in

parental *T. b. rhodesiense* STIB900 localized to a (silent) telomeric VSG expression site rather than to the chromosome-internal or minichromosomal VSG repository (El-Sayed *et al.*, 2000). The suramin resistance phenotype was slowly reversible over time, which might be explained by the slightly longer population doubling times of the resistant derivatives.

The causality between VSG^{Sur} expression and suramin resistance was confirmed by reverse genetic re-introduction of the originally expressed VSG into the resistant parasites, which completely restored susceptibility. The finding that the expression of VSG^{Sur} causes suramin resistance, explains the fast emergence of the resistance and the high reproducibility of the *in vitro* selection. It also explains the discrepancy with Hawking's observation cited above, because he was using subcurative treatment of infected mice to select for resistance (*in vitro* cultivation of *T. brucei* was not possible at the time).

In vivo, parasites that are bound to express a particular VSG under suramin pressure will be eliminated by host antibodies. This might be the reason why suramin, after one century of use, is still effective in the treatment of early-stage east-African sleeping sickness. The commonly used regimen is five injections of 20 mg kg⁻¹, leading to suramin plasma levels over 100 µg ml⁻¹ for several weeks (Burri *et al.*, 2004), which is clearly above the *in vitro* IC₅₀ of trypanosomes expressing VSG^{Sur}. The situation would be different if lower doses of suramin were administered. One could speculate that such a mechanism could have facilitated the emergence of suramin resistance in animal-pathogenic trypanosomes, as the usual treatment regimen in horses and camels is a single dose of 10 mg kg⁻¹ suramin, and the disease typically leads to immunosuppression (Giordani *et al.*, 2016). Thus if the trypanosomes escaped the effects of suramin in the short term by switching to a certain VSG, this would give them more time to develop other resistance mechanisms. It has been reported that a functional immune system is important for effective suramin treatment of animal trypanosomiasis (Leach and Roberts, 1981).

VSGs could be either directly or indirectly involved in binding and uptake of suramin, and VSG^{Sur} might be non-functional in this respect. Previous studies which proposed an uptake of suramin via endocytosis (Fairlamb and Bowman, 1980; Vansterkenburg *et al.*, 1993) are in accordance with this, as VSG in *T. brucei* bloodstream forms is endocytosed at a very high rate (Engstler *et al.*, 2004). An involvement of VSG in suramin binding or uptake could also explain the insensitivity of procyclic trypanosomes to suramin (Scott *et al.*, 1996) as they do not express VSG genes.

Binding of trypan blue at 4°C to suramin-sensitive trypanosomes suggests a saturable high-affinity component

plus a low affinity component that becomes apparent at 390 µg ml⁻¹ trypan blue (testing of higher concentrations was not possible because of toxicity and solubility problems). This implies the presence of more than one binding partner on the cell surface of the sensitive clone. The low affinity component appeared to be missing in the suramin-resistant clones (Fig. 7B). However, the uptake of trypan blue at 37°C by the suramin-resistant lines was impaired at concentrations between 5 and 200 µg ml⁻¹ (Fig. 7C), indicating that the low-affinity binding component may not be responsible for drug resistance. Thus while the genetic basis for fast suramin resistance in *T. brucei* is an expression switch to VSG^{Sur}, the biochemical basis remains to be elucidated.

Experimental procedures

T. brucei isolates and cultivation

The *T. b. rhodesiense* strain STIB900 is a derivative of STIB704, which was originally isolated from a male patient at St. Francis Hospital in Ifakara, Tanzania in 1982. It was passaged several times in rodents and once in a tsetse fly (*Glossina morsitans morsitans*) before a cloned population was adapted to axenic *in vitro* culture. *T. brucei* BS221 was received from Dr. Sam Black, International Laboratory for Research on Animal Diseases (ILRAD, Kenya). Parasites were cultivated in Iscove's Modified Dulbecco's Medium supplemented according to Hirumi (Hirumi and Hirumi, 1989) with 15% of heat-inactivated horse-serum. The parasites were grown at 37°C, 5% CO₂ and diluted three times a week.

Microcalorimetry with *T. b. rhodesiense*

T. b. rhodesiense strain STIB900 were cultivated in Minimum Essential Medium with Earle's salts, supplemented according to Baltz *et al.* (Baltz *et al.*, 1985) with minor modifications: 0.2 mM 2-mercaptoethanol, 1 mM sodium pyruvate, 0.5 mM hypoxanthine and 15% heat-inactivated horse serum. Trypanosome cultures in the late exponential growth phase were diluted with fresh culture medium to a density of 10⁵ cells ml⁻¹. Ampoules were filled, in triplicate, with 3 ml cell suspension and supplemented with suramin, pentamidine or melarsoprol at concentrations corresponding to 5 × IC₅₀ or 25 × IC₅₀ in the identical medium (Wenzler *et al.*, 2012). Culture medium without trypanosomes served as baseline control. The heat flow was measured continuously over a period of 8 days at 37°C in a TAM III isothermal microcalorimeter (thermal activity monitor, model 249; TA instruments, New Castle DE, USA).

Cloning of *T. b. rhodesiense*

A microdrop of a suspension with 10⁴ cells ml⁻¹ was made using a gilded paperclip and inspected by two persons under an inverted microscope. After confirmation of the

presence of a single cell, the microdrop was supplemented with 50 μl of cloning medium. This consisted of 59% Iscove's modified Dulbecco's Medium, which had been supplemented according to Hirumi (Hirumi and Hirumi, 1989) for a total volume of 100%, 1% Mäser-mix (Mäser *et al.*, 2002), 20% inactivated horse-serum and 20% of pre-conditioned medium. The pre-conditioned medium was prepared by centrifugation of a dense trypanosome culture (10 min at 1840 g) and subsequent sterile filtering of the supernatant. After four days of incubation at 37°C, 5% CO₂, the plate was inspected under an inverted microscope and 50 μl of cloning medium was added to the wells with a growing clonal colony. After another 3 days the clones were passaged to new plates and cultivated as described above.

In vitro selection for drug resistance and determination of growth rates

A fresh clone of *T. b. rhodesiense* STIB900 in the exponential growth phase was selected with 1050 nM suramin in four wells each containing 1 ml medium with 5×10^4 cells. After 6 days the parasites were removed from drug pressure by washing three times with fresh culture medium and cultured in drug-free medium as described above. For the BS221 strain 10^5 cells were selected with 1070 nM (BS221_sur1) and 4270 nM (BS221_sur2) suramin and removed from drug pressure after 5 days. Cell growth was measured between day 15 and day 26 after selection. Cumulative growth curves were determined by dilution of the cells to 10^5 ml^{-1} , incubation for 24 h, and measurement of cell density with a CASY Cell Counter (OMNI Life Science, Bremen). This procedure was repeated for four days. Cumulative cell numbers and the population doubling times were calculated and statistically evaluated with t-tests applying Benjamini-Hochberg correction using R Studio (R version 3.3.3).

Alamar blue assay

Suramin sodium salt and pentamidine isethionate were obtained from Sigma (S2671 and P0547 respectively), Trypan Blue from Fluka (93590) and melarsoprol from Sanofi-Aventis/WHO. Alamar blue assays (Räz *et al.*, 1997) for determination of *in vitro* drug sensitivities were carried out at least three times independently. Serial drug dilutions were prepared on a 96 well plate in technical duplicates and cells were added in a concentration of 2×10^4 . Parasite-free, drug-free wells were used for determination of background fluorescence. After an incubation time of 69 h, plates were inspected microscopically and resazurin was added to a final concentration of 36 μM . Fluorescence intensity was measured after 3–4 h incubation using a SpectraMax (Molecular Devices) and SoftMax Pro 5.4.5 software. The 50% inhibitory concentrations (IC₅₀) were calculated with GraphPad Prism 6.00 using a non-linear regression model to fit the dose-response curve (variable slope; four parameters, bottom value set to zero). Statistical analysis was performed with GraphPad Prism 6.00 using an ordinary one-way ANOVA with Tukey's multiple comparisons test.

Extraction of RNA, mRNA-seq and comparative transcriptomics

Cultures in the exponential growth phase were centrifuged and washed once with PBS before total RNA was isolated using the RNeasy Mini Kit (Qiagen) including an on-column DNase treatment. RNA was shock-frozen in liquid nitrogen and stored at -80°C . Five microgram of RNA from two independent isolations were pooled for each sample. Library preparation and sequencing was performed at the Quantitative Genomics Facility (QGF) of the ETH Zurich in Basel. Sequencing libraries were prepared using the TruSeq Stranded mRNA Library preparation kit (Illumina). Single-end sequencing of 125 nucleotides was carried out on an illumina HiSeq 2500. The bioinformatic analysis was carried out on the sciCORE cluster of the University of Basel. Quality of the sequencing reads was controlled with fastqc software (Babraham Bioinformatics - FastQC A Quality Control tool for High Throughput Sequence Data. Available at: <http://www.bioinformatics.babraham.ac.uk/projects/fastqc/>. Accessed: 6th April 2017). Illumina adaptors, low quality ends and reads with a length of fewer than 36 nucleotides were removed with trimmomatic (Bolger *et al.*, 2014). Sequencing reads were mapped to the TREU927 reference genome (version TriTrypDB-28) complemented with bloodstream expression sites from Lister427 (Hertz-Fowler *et al.*, 2008). Mapping was performed with bwa (Li and Durbin, 2009) using the default parameters (seedlength of 19 nucleotides, matching score of 1, mismatch penalty of 4, gap open penalty of 6 and a gap extension penalty of 1). The alignment files in the SAM format were converted to binary files using samtools (Li *et al.*, 2009) and sorted and indexed using picard tools (Broad Institute. Available at: <http://broad-institute.github.io/picard/>. Accessed: 6th April 2017). Read counts per transcript were determined with the Python package HTSeq (Anders *et al.*, 2015) using a combined gff file from TREU927 (version TriTrypDB-28) and bloodstream expression sites from Lister427 (Hertz-Fowler *et al.*, 2008), default parameters with a minimal mapping quality of 10 were used. Raw counts were analyzed with the R package DESeq2 (Love *et al.*, 2014) (version 1.14.1), independent filtering was disabled.

The *de novo* assembly of transcripts was carried out using trinity (Grabherr *et al.*, 2011) with the default parameters. The *de-novo* assembled transcripts were screened with blastn for ESAG7-like genes using the sequence of gene Tb927.7.3260 as query.

Reverse transcription, PCR and quantitative PCR

Complementary DNA (cDNA) was synthesized with SuperScript III Reverse Transcriptase (Invitrogen via Thermo Fisher Scientific, Waltham MA, USA) according to the manufacturer's protocol using oligo(dT) primer and 1–5 μg of total RNA. One microliter of the 1:100 diluted cDNA was used for PCR. Amplification of the VSGs was performed with one primer binding to the spliced leader sequence (Parsons *et al.*, 1984) at the 5' UTR and the other primer binding to the 3' end of the gene (Supporting Information Table S1). The sequences of the 3'ends were derived from the *de-novo* assembly. For amplification of the VSG

expressed in the BS221 strain, a primer binding unspecifically to the 3' ends of all VSGs (Aline *et al.*, 1985) was used (Supporting Information Table S1). The PCR was carried out with Taq polymerase (Solis BioDyne, Estonia) or with KAPA HiFi HotStart DNA Polymerase (Kapa Biosystems, Cape Town, South Africa). PCR products were run on a 1% agarose gel, which was subsequently stained with GelRed Nucleic Acid Gel Stain (Biotium, Fremont CA, USA). The PCR products were purified with the Wizard SV Gel and PCR Clean-Up System (Promega, Madison WI, USA) or the NucleoSpin Gel and PCR Clean-up (Macherey-Nagel, Düren, Germany) and sent to Microsynth (Balgach, Switzerland) for sequencing. Primers for sequencing were the same as used for PCR, additional internal primers were designed for completion of the sequences. Quantitative PCR was carried out with Power SYBR Green (Applied Biosystems via Thermo Fisher Scientific) on a StepOnePlus real-time PCR System (Applied Biosystems) in technical duplicates. StepOne Software v2.3 was used for analysis of the amplification plots and calculation of the C_T values, which were normalized to the housekeeping gene telomerase reverse transcriptase (Brenndörfer and Boshart, 2010) (*TERT*; ΔC_T). All primers (Supporting Information Table S1) were designed using the Primer3Plus software (Available at: <http://primer3plus.com/cgi-bin/dev/primer3plus.cgi>. Accessed: 6th April 2017)

Reverse genetics with *T. brucei*

For the gene exchange of *VSG^{Sur}* to *VSG⁹⁰⁰* a construct was designed (Fig. 5A) containing the 3' and 5' UTRs of *VSG^{Sur}*, the coding sequence of *VSG⁹⁰⁰*, an $\alpha\beta$ tubulin splice site and a blasticidin-resistance gene (BSD). The DNA was synthesized by GenScript (Piscataway Township NJ, USA) and integrated between the HindIII and the EcoRI-site of a pUC57 vector. For amplification of the insert a PCR was performed using two flanking primers. Three microgram of the purified PCR product were used for the transfection of 4×10^7 STIB900_c1_sur1 cells in 100 μ l Tb-BSF buffer (Schumann Burkard *et al.*, 2011) with an Amaxa Nucleofector using program Z-001. Positive transfected clones were obtained by limiting dilution in standard culture medium. After 24 h of incubation, blasticidin was added to a total concentration of 5 μ g ml^{-1} . The construct integration was verified by PCR on genomic DNA: As the flanking genomic sequences upstream and downstream of *VSG^{Sur}* are unknown, primers binding to the 5' and 3' UTR of *VSG^{Sur}* were used for the PCR (Fig. 5), which resulted in a band of 1624 nucleotides derived from the wildtype sequence of *VSG^{Sur}* and a second band of 2356 nucleotides in the presence of the construct. Genomic DNA was isolated from 10 ml dense culture in the following manner: The culture was centrifuged at 1800 g for 5 min and washed with TE buffer (10 mM TrisHCl pH 8, 1 mM EDTA) once. Cells were eluted in 100 μ l TE buffer and lysed by addition of 1 μ l of 10% SDS and incubation for 10 min at 55°C. Subsequently 30 μ l of 5 M potassium acetate were added to the lysate and incubated on ice for 5 min to precipitate SDS and proteins. The lysate was spun down for 5 min at full speed in a microcentrifuge and the supernatant

transferred to a new tube. The DNA was precipitated with absolute ethanol, washed with 70% ethanol and eluted in 20 μ l H_2O . PCR was carried out as described above. The expression of *VSG^{Sur}* and *VSG⁹⁰⁰* was measured by quantitative PCR as described above.

Trypan blue binding and uptake

A total of 2×10^5 parasites per sample was exposed to trypan blue (5, 20, 50, 200 or 390 μ g ml^{-1}) in 1 ml standard growth medium and incubated for two hours at 37°C or 4°C. After incubation, the parasites were centrifuged (5 min, 3000 g) and washed twice with 1 ml PBS (Phosphate-buffered saline; 137 mM NaCl, 2.7 mM KCl, 10 mM Na_2HPO_4 , 1.8 mM KH_2PO_4 , pH 7.4) at room temperature or 4°C respectively. The cells were resuspended in 250 μ l PBS followed by the addition of 250 μ l 10% formalin for fixation. The fluorescence intensity of the fixed cells was measured with a BD FACSCalibur™ flow cytometer (BD Biosciences, San Jose, CA, USA) using the FL3 channel (670 nm long pass) upon excitation at 488 nm. Ten thousand events were acquired within the parasite gate based on size versus granularity (FSC x SSC). Dot plots and their fluorescence were evaluated in FL3 histograms as trypan blue has its emission peak at 660 nm (Avelar-Freitas *et al.*, 2014). The measured fluorescence intensity was analyzed with Flowing Software (Version 2.5.1) by using a living parasite gate based on size versus fluorescence intensity (FSC x FL3) and statistically evaluated with R Studio, applying pairwise t-tests (Version 1.0.143, R version 3.3.3).

Acknowledgements

We are most grateful to Sebastian Hutchinson for helpful advice, to the Genomics Facility of the ETHZ in Basel for sequencing, to sciCORE of the University of Basel for data analysis runtime, and to Françoise Brand and Henning Stahlberg for the scanning electron microscopy picture. This study was funded by the Swiss National Science Foundation (Schweizerischer Nationalfonds zur Förderung der Wissenschaftlichen Forschung grants 31003A_135746 and 310030_156264).

Conflict of Interest

The authors declare no conflict of interest.

Author contributions

NW i, ii, iii; FG i, ii; MZ i, ii; EN ii; CK ii; MC ii; RS i; TW i, ii; PM i, iii

References

Aline, R., MacDonald, G., Brown, E., Allison, J., Myler, P., Rothwell, V., and Stuart, K. (1985) (TAA)_n within

- sequences flanking several intrachromosomal variant surface glycoprotein genes in *Trypanosoma brucei*. *Nucleic Acids Res* **13**: 3161–3177.
- Alsford, S., Eckert, S., Baker, N., Glover, L., Sanchez-Flores, A., Leung, K.F., *et al.* (2012) High-throughput decoding of antitrypanosomal drug efficacy and resistance. *Nature* **482**: 232–236.
- Alsford, S., Field, M.C., and Horn, D. (2013) Receptor-mediated endocytosis for drug delivery in African trypanosomes: fulfilling Paul Ehrlich's vision of chemotherapy. *Trends Parasitol* **29**: 207–212.
- Anders, S., Pyl, P.T., and Huber, W. (2015) HTSeq—a Python framework to work with high-throughput sequencing data. *Bioinforma Oxf Engl* **31**: 166–169.
- Avelar-Freitas, B.A., Almeida, V.G., Pinto, M.C.X., Mourão, F. A G., Massensini, A.R., Martins-Filho, O.A., *et al.* (2014) Trypan blue exclusion assay by flow cytometry. *Braz J Med Biol Res Rev Bras Pesqui Medicas E Biol* **47**: 307–315.
- Baltz, T., Baltz, D., Giroud, C., and Crockett, J. (1985) Cultivation in a semi-defined medium of animal infective forms of *Trypanosoma brucei*, *T. equiperdum*, *T. evansi*, *T. rhodesiense* and *T. gambiense*. *EMBO J* **4**: 1273–1277.
- Bernhard, S.C., Nerima, B., Mäser, P., and Brun, R. (2007) Melarsoprol- and pentamidine-resistant *Trypanosoma brucei* rhodesiense populations and their cross-resistance. *Int J Parasitol* **37**: 1443–1448.
- Bolger, A.M., Lohse, M., and Usadel, B. (2014) Trimmomatic: a flexible trimmer for Illumina sequence data. *Bioinforma Oxf Engl* **30**: 2114–2120.
- Brenndörfer, M., and Boshart, M. (2010) Selection of reference genes for mRNA quantification in *Trypanosoma brucei*. *Mol Biochem Parasitol* **172**: 52–55.
- Brickman, M.J., Cook, J.M., and Balber, A.E. (1995) Low temperature reversibly inhibits transport from tubular endosomes to a perinuclear, acidic compartment in African trypanosomes. *J Cell Sci* **108**: 3611–3621.
- Burri, C., Stich, A., and Brun, R. (2004) Current Chemotherapy of Human African Trypanosomiasis. In *The Trypanosomiasis*. Maudlin, I., Holmes, P.H., and Miles, M.A. (eds). CABI Publishing, p. 403.
- El Rayah, I.E., Kaminsky, R., Schmid, C., and El Malik, K.H. (1999) Drug resistance in Sudanese *Trypanosoma evansi*. *Vet Parasitol* **80**: 281–287.
- El-Sayed, N.M., Hegde, P., Quackenbush, J., Melville, S.E., and Donelson, J.E. (2000) The African trypanosome genome. *Int J Parasitol* **30**: 329–345.
- Engstler, M., Thilo, L., Weise, F., Grünfelder, C.G., Schwarz, H., Boshart, M., and Overath, P. (2004) Kinetics of endocytosis and recycling of the GPI-anchored variant surface glycoprotein in *Trypanosoma brucei*. *J Cell Sci* **117**: 1105–1115.
- Fairlamb, A.H., and Bowman, I.B. (1980) Uptake of the trypanocidal drug suramin by bloodstream forms of *Trypanosoma brucei* and its effect on respiration and growth rate in vivo. *Mol Biochem Parasitol* **1**: 315–333.
- Fang, Y., Ye, W.X., Nei, H.Y., and Wang, Y.L. (1994) In vitro development of suramin-resistant clones of *Trypanosoma evansi*. *Acta Trop* **58**: 79–83.
- Fankhauser, N., and Mäser, P. (2005) Identification of GPI anchor attachment signals by a Kohonen self-organizing map. *Bioinforma Oxf Engl* **21**: 1846–1852.
- Giordani, F., Morrison, L.J., Rowan, T.G., DE Koning, H.P., and Barrett, M.P. (2016) The animal trypanosomiasis and their chemotherapy: a review. *Parasitology* **143**: 1862–1889.
- Grabherr, M.G., Haas, B.J., Yassour, M., Levin, J.Z., Thompson, D.A., Amit, I., *et al.* (2011) Full-length transcriptome assembly from RNA-Seq data without a reference genome. *Nat Biotechnol* **29**: 644–652.
- Hawking, F. (1963) Chemotherapy of Trypanosomiasis. In *Experimental chemotherapy*. Schnitzer, R.J., and Hawking, F. (eds). Academic Press.
- Hertz-Fowler, C., Figueiredo, L.M., Quail, M.A., Becker, M., Jackson, A., Bason, N., *et al.* (2008) Telomeric expression sites are highly conserved in *Trypanosoma brucei*. *PLoS One* **3**: e3527.
- Hirumi, H., and Hirumi, K. (1989) Continuous cultivation of *Trypanosoma brucei* blood stream forms in a medium containing a low concentration of serum protein without feeder cell layers. *J Parasitol* **75**: 985–989.
- Leach, T.M., and Roberts, C.J. (1981) Present status of chemotherapy and chemoprophylaxis of animal trypanosomiasis in the Eastern hemisphere. *Pharmacol Ther* **13**: 91–147.
- Li, H., and Durbin, R. (2009) Fast and accurate short read alignment with Burrows-Wheeler transform. *Bioinforma Oxf Engl* **25**: 1754–1760.
- Li, H., Handsaker, B., Wysoker, A., Fennell, T., Ruan, J., Homer, N., *et al.* (2009) The Sequence Alignment/Map format and SAMtools. *Bioinforma Oxf Engl* **25**: 2078–2079.
- Love, M.I., Huber, W., and Anders, S. (2014) Moderated estimation of fold change and dispersion for RNA-seq data with DESeq2. *Genome Biol* **15**: 550.
- Luenen, H.G.A.M., van, Kieft, R., Musmann, R., Engstler, M., Riet, B. T., and Borst, P. (2005) Trypanosomes change their transferrin receptor expression to allow effective uptake of host transferrin. *Mol Microbiol* **58**: 151–165.
- Mäser, P., Grether-Bühler, Y., Kaminsky, R., and Brun, R. (2002) An anti-contamination cocktail for the in vitro isolation and cultivation of parasitic protozoa. *Parasitol Res* **88**: 172–174.
- Nielsen, H., Engelbrecht, J., Brunak, S., and Heijne, G. von. (1997) A neural network method for identification of prokaryotic and eukaryotic signal peptides and prediction of their cleavage sites. *Int J Neural Syst* **8**: 581–599.
- Parsons, M., Nelson, R.G., Watkins, K.P., and Agabian, N. (1984) Trypanosome mRNAs share a common 5' spliced leader sequence. *Cell* **38**: 309–316.
- Pépin, J., and Milord, F. (1994) The treatment of human African trypanosomiasis. *Adv Parasitol* **33**: 1–47.
- Rätz, B., Iten, M., Grether-Bühler, Y., Kaminsky, R., and Brun, R. (1997) The Alamar Blue assay to determine drug sensitivity of African trypanosomes (*T.b. rhodesiense* and *T.b. gambiense*) in vitro. *Acta Trop* **68**: 139–147.
- Schumann Burkard, G., Jutzi, P., and Roditi, I. (2011) Genome-wide RNAi screens in bloodstream form trypanosomes identify drug transporters. *Mol Biochem Parasitol* **175**: 91–94.
- Scott, A.G., Tait, A., and Turner, C.M. (1996) Characterisation of cloned lines of *Trypanosoma brucei* expressing stable resistance to MelCy and suramin. *Acta Trop* **60**: 251–262.

- Vansterkenburg, E.L., Coppens, I., Wilting, J., Bos, O.J., Fischer, M.J., Janssen, L.H., and Opperdoes, F.R. (1993) The uptake of the trypanocidal drug suramin in combination with low-density lipoproteins by *Trypanosoma brucei* and its possible mode of action. *Acta Trop* **54**: 237–250.
- Wang, C.C. (1995) Molecular mechanisms and therapeutic approaches to the treatment of African trypanosomiasis. *Annu Rev Pharmacol Toxicol* **35**: 93–127.
- Wenzler, T., Steinhuber, A., Wittlin, S., Scheurer, C., Brun, R., and Trampuz, A. (2012) Isothermal microcalorimetry, a new tool to monitor drug action against *Trypanosoma brucei* and *Plasmodium falciparum*. *PLoS Negl Trop Dis* **6**: e1668.
- Zhou, J., Shen, J., Liao, D., Zhou, Y., and Lin, J. (2004) Resistance to drug by different isolates *Trypanosoma evansi* in China. *Acta Trop* **90**: 271–275.

Supporting information

Additional supporting information may be found in the online version of this article at the publisher's web-site.